

# Integration of RF-MEMS Switches with a Band-Reject Reconfigurable Ultra-Wideband Antenna on $\text{SiO}_2$ Substrate

Nelson Sepulveda<sup>(1)</sup>, Dimitris E. Anagnostou<sup>(2)\*</sup>,  
Michael T. Chryssomallis<sup>(3)</sup> and John L. Ebel<sup>(4)</sup>

<sup>(1)</sup> ECE Dept., University of Puerto Rico at Mayagüez, Mayagüez, 00681, PR, USA

<sup>(2)</sup> ECE Dept., South Dakota School of Mines & Tech., Rapid City, 57701, SD, USA

<sup>(3)</sup> ECE Department, Democritus University of Thrace, Xanthi, 67-100, Greece

<sup>(4)</sup> Air Force Research Laboratories, Wright-Patterson Air-Force Base, OH, 45433

\*E-mail: danagn@ieee.org

## Introduction

An ultra-wideband reconfigurable antenna for WLAN environments integrated with RF-MEMS switches is presented. Using MEMS, the antenna rejects *on-demand* the 5-6 GHz WLAN 802.11a frequency band. The design is integrated on-wafer with MEMS switches and high-resistive biasing lines to minimize interference of the packaging and allow biasing through the designed bias pads. The antenna's design procedure, fabrication and measured reflection coefficient are described. Results show satisfactory band-rejection quality and (most-important), very little interference of the MEMS and biasing circuitry with the antenna itself. Such designs can be used in low-loss future UWB antennas that minimize interference to nearby WLAN receivers.

Reconfigurable antenna systems have been theorized in the past decade [1]. Such systems provide multifunctionality to a device, with most being related to the antenna's resonant frequencies [2], polarization [3] and radiation pattern [4]. Although a plethora of works describes reconfigurable antenna systems, few describe the fabrication and integration procedure of the antenna with an integrated reconfiguration mechanism. Some of the first ultra-wideband antennas with simple, single-band-reject and dual-band-reject mechanisms can be found in [5] and [6] respectively. Such antennas find applications in UWB systems for the rejection or minimization of the part of the UWB transmitted spectrum that interference with existing US and worldwide WLAN and U-NII networks within the 5.15-5.35 GHz, 5.47-5.725 GHz and 5.725-5.825 GHz bands. The on-demand rejection of interfering frequencies leads to higher system capacity, minimum WLAN interference with maximum throughput and battery lifetime through the intelligent use of the band-reject mechanism. However, such a device has not been implemented yet because of two major complexities:

- 1) Low-cost switching mechanisms (e.g. high-frequency p-i-n diodes) would incur losses to the already low-power UWB transmitted signal and would distort the UWB pulses due to their non-linearity, thus interacting with the transmitted signal to the point that their usage is impractical.
- 2) The majority of UWB antennas are made as planar monopoles and the biasing of a MEMS switching mechanism cannot be accomplished with the commonly used quarter-wavelength lines and stubs.

In this work, these complexities are resolved successfully and the monolithic integration of MEMS with a band-reject UWB antenna is achieved using standard cleanroom photolithography procedures. The *MEMS-reconfigurable UWB*

antenna that is proposed, is fabricated and measured, and results are presented. What distinguishes this work from others (e.g. [2]) is the utilized materials and substrate (low-cost  $\text{SiO}_2$  instead of expensive high-resistive  $\text{Si}$ ) and the new application (on-demand band-rejection instead of multi-frequency).

### RF-MEMS Design and Integration with the Antenna

The designed UWB antenna consists of a flattened UWB monopole fed through a tapered (to minimize losses) coplanar waveguide-fed (CPW) radiating element with two extended ground patches on the side as shown in Fig. 1. The radiating element has two RF-MEMS switches ('A' and 'B') connected symmetrically on its sides at a distance where the RF current at 5.5 GHz is maximized. This frequency is the middle of the cutoff band. The MEMS switches are biased through  $\text{Ti-Au}$  high-resistive bias lines that exist on the switch area only, and thus do not interfere with the RF current of the antenna. The bias lines extend at the top of the antenna to three  $400\mu\text{m}$  pitch DC-pads that allow the biasing of the switches on the  $\text{SiO}_2$  with minimal interference to the antenna's radiation pattern, for the reason that the antenna exhibits low radiation toward that direction.

The MEMS connect two open-ended quarter-wavelength stubs to the antenna. The stubs appear as short-circuits to the 5.5 GHz current of the switch, and thus 'resonate' with a surface current density of opposite direction to the surface current at the edges of the patch. In this way, they create a low-impedance point at the switch that allows RF current flow, while creating a VSWR mismatch at the input. The MEMS bias network allows two useful stub configuration states as shown (in dark gray color) in Fig. 2(a-b): a traditional UWB 'OFF'-mode antenna and a 'reconfigurable' band-reject 'ON' mode antenna.

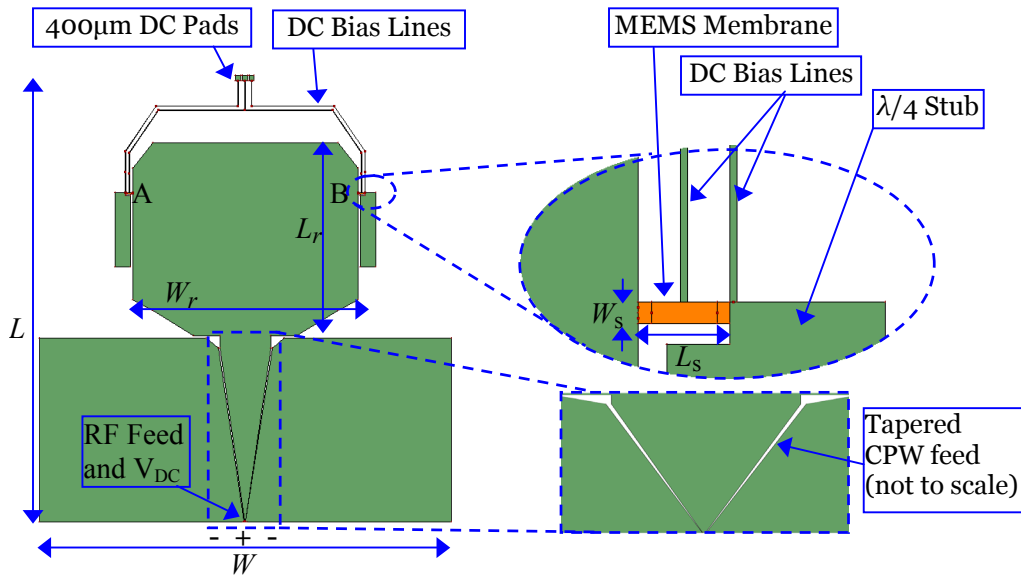


Fig. 1. Simulated model of the band-reject UWB antenna showing the placement of the integrated RF-MEMS switches.

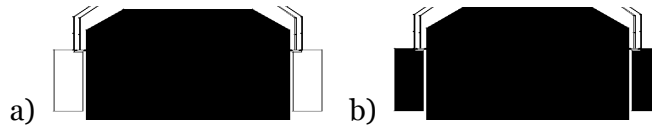


Fig. 2(a-b). a) 'OFF' and b) 'ON' antenna configurations. (not to scale).

The radiating element is only  $W_r \times L_r = 22 \times 25.5\text{mm}$ , while the entire structure is  $W \times L = 40.2 \times 53.75\text{mm}$ . The MEMS switches are of ohmic contact cantilever type and their dimensions are only  $L_s \times W_s = 660 \times 175 \mu\text{m}$ . An electrostatic pull-down (actuation) voltage of 70 volts was used to flex the membrane enough for the RF current to pass through.

The antenna and the switches were fabricated on a 4-inch  $\text{SiO}_2$  substrate and both shared a single fabrication process flow. First, a  $\text{Ti-Au}$  layer was deposited and patterned by a lift-off process. The  $\text{Ti}$  served only as an adhesion layer and was 20 nm thick. The  $\text{Au}$  layer was initially 280 nm, but this thickness was subsequently increased to  $5.5 \mu\text{m}$  by electroplating. Then, the antenna and MEMS bottom electrode layer was patterned. The subsequent fabrication steps are only for the RF MEMS. A second mask was used to pattern the resistive layer that would isolate the DC bias lines from the RF lines. For the resistive layer's DC Bias Lines, a  $1000 \text{ \AA}$   $\text{W-SiO}$  film was sputtered and patterned by lift-off as well. A third mask was used to pattern the switch posts, while the fourth defined the dimples that were used to minimize stiction problems, and the fifth mask defined the switch bridge or membrane. The sacrificial layer used for the switches was a Polymethylglutarimide (PMGI) layer; and its removal was done as the last fabrication step by IPA, methanol, and  $\text{CO}_2$  drying. It is important to note that using this single fabrication of MEMS procedure, the antenna, the MEMS and the biasing network were fabricated and integrated into a single device.

### Measurements and Results

The frequency response of the antenna was measured at the Re-Configurable Antenna Measurement Platform (ReCAMP) at the South Dakota School of Mines and Technology. A photo of the fabricated antenna during measurement, placed over Styrofoam spacer is shown in Fig. 3. The measured results for both configurations (MEMS 'ON' and MEMS 'OFF') are shown in Fig. 4 and are compared with simulated using the suitable for planar structures, Zeland IE3D™.

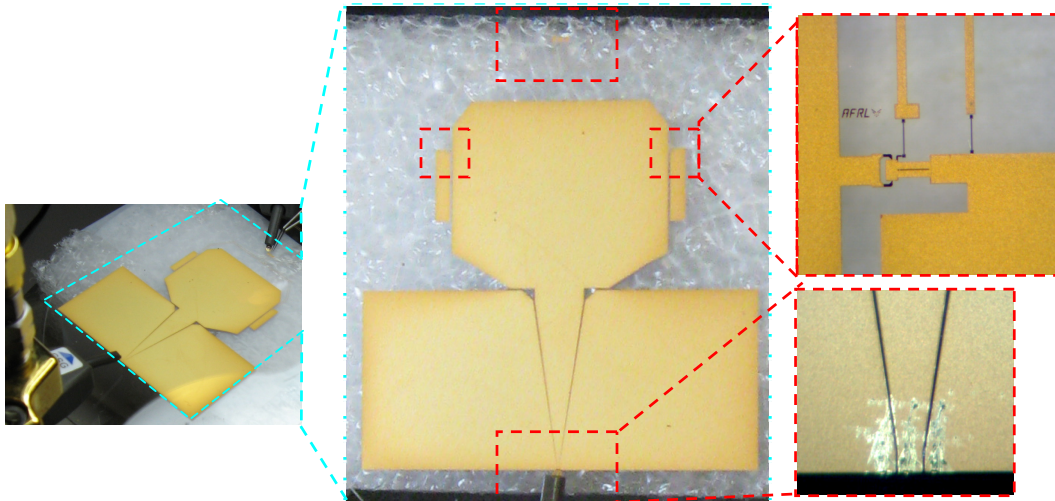


**Fig. 3.** Photo of the fabricated antenna with integrated MEMS during measurements, showing the RF-probe (bottom) and DC bias pads (top). The MEMS, DC lines and RF feed are in the microscope photo (right).

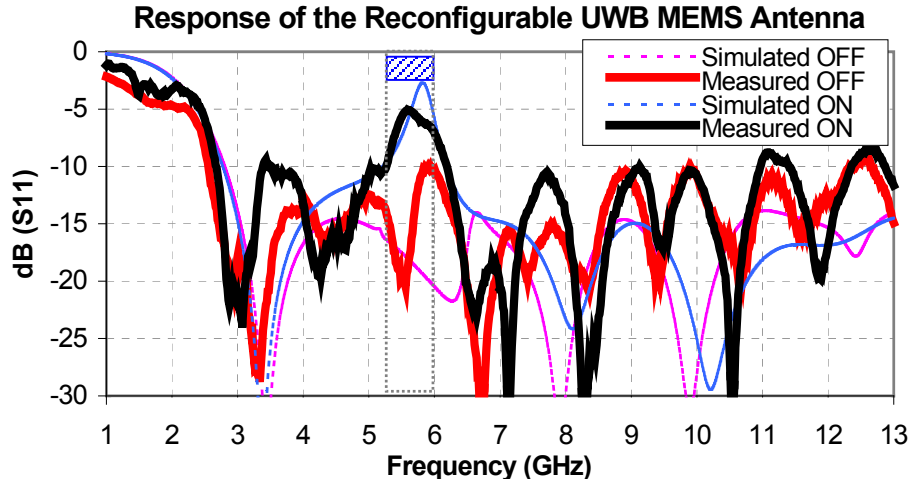


**Fig. 4. Return loss of the integrated UWB MEMS antenna. Notice the relatively high cutoff ( $|S_{11}| > -7\text{dB}$ ) in the 5.25-5.775GHz WLAN rejected range.**

Even though there is substantial equipment around the antenna to measure it (i.e. a probe station chuck and RF and DC probes), their interference appears to be minimal on the antenna response. Also, the proper modeling and subsequent integration of the MEMS minimized any effects they could possibly have with the antenna itself and limits their functionality to the band-rejection mechanism only. Results show that for the switches 'OFF', the antenna is a traditional UWB antenna that covers a superset of the typical 3.1-10.6 GHz band with VSWR < 2. When the DC voltage is applied, the switches turn 'ON' and the antenna becomes a frequency band-notched selective UWB antenna that rejects the 5.15-5.825GHz range of frequencies that includes both the WLAN 802.11a band and the intermediate U-NII band in the 5.47-5.725GHz range.

### Acknowledgement

This work was supported in part by DoD ARO Grant No. W911NF-09-1-0277, by NASA #NNX07AL04A, by MacAulay-Brown, Inc. #MacB-07-D-0016/0010, by the NSF Grant #HRD-0833112 and NSF/EPSCoR Grant #EPS-0903804.

### References

- [1] E. R. Brown, "RF-MEMS Switches for Reconfigurable Integrated Circuits", *IEEE Trans. Microwave Theory Tech.*, V. 46, Is. 11, pp. 1868-80, Nov. 1998.
- [2] D. E. Anagnostou, G. Zheng, M. Chryssomallis, J. Lyke, G. Ponchak, J. Papapolymerou, and C. G. Christodoulou, "Design, Fabrication and Measurements of an RF-MEMS-Based Self-Similar Reconfigurable Antenna", *IEEE Trans. Antennas and Prop.*, V. 54, Is. 2, Pt 1, pp: 422-432, Feb 2006.
- [3] R. N. Simons, D. Chun and L. P. B. Katehi, "Polarization reconfigurable patch antenna using microelectromechanical systems (MEMS) actuators," *IEEE APS/URSI Intl' Symp.*, v.1, pp.6-9, June 2002.
- [4] G. H. Huff and J. T. Bernhard, "Integration of packaged RF MEMS switches with radiation pattern reconfigurable square spiral microstrip antennas," *IEEE Trans. on Antennas and Prop.*, v. 54, pp. 464-469, Feb. 2006.
- [5] H. G. Schantz, G. Wolenc, E. M. Myszka, "Frequency notched UWB antennas", *IEEE Conf. on UWB Systems & Tech.*, VA, 16-19 Nov. 2003, pp: 214-218.
- [6] D. E. Anagnostou et. al., "Dual Band-Notched Ultra-Wideband Antenna for 802.11a LAN Environments", *IEEE APS/URSI Intl' Symp.*, June 10-15, 2007, pp. 4621-4624.